Journal of Molecular Catalysis A: Chemical 329 (2010) 50–56

Contents lists available at ScienceDirect

Journal of Molecular Catalysis A: Chemical

journal homepage: www.elsevier.com/locate/molcata

Effect of the support on the catalytic properties of vanadyl phosphate in the oxidative dehydrogenation of propane

M.P. Casaletto[a], G. Landi[b,*], L. Lisi[b], P. Patrono[c], F. Pinzari[c]

[a] Istituto per lo Studio dei Materiali Nanostrutturati, CNR, Via U. La Malfa 153, 90146 Palermo, Italy
[b] Istituto di Ricerche sulla Combustione, CNR, P.le Tecchio 80, 80125 Naples, Italy
[c] Istituto di Metodologie Inorganiche e dei Plasmi, CNR, Monterotondo Scalo, Italy

ARTICLE INFO

Article history:
Received 15 January 2010
Received in revised form 8 June 2010
Accepted 16 June 2010
Available online 23 June 2010

Keywords:
Propane
Oxidative dehydrogenation
Vanadium phosphate

ABSTRACT

Propane oxidative dehydrogenation has been investigated on vanadyl orthophosphate dispersed on different supports (Al_2O_3, TiO_2, SiO_2, ZrO_2, MgO and SnO) in a fixed bed reactor in the temperature range 300–550 °C. Catalysts have been characterized by bulk and surface sensitive techniques, such as X-ray diffraction (XRD), BET analysis, temperature programmed reduction with H_2 (H_2-TPR) and X-ray photoelectron spectroscopy (XPS). A different dispersion of vanadium species has been found depending on the different nature of the supports. Al_2O_3, ZrO_2 and TiO_2 promote the best dispersion of vanadium and provide the highest catalytic performances, due to the strong interaction of the support with the phosphate phase and the enhanced vanadium reducibility. A different reaction path is activated by catalysts supported on SiO_2, MgO and SnO due to the formation of vanadyl phosphate aggregates and in some cases also to the reducibility of the support which favour propane overoxidation leading to a larger CO_2 production.

1. Introduction

During the last years the interest for the selective oxidation of light hydrocarbons has remarkably grown. As a matter of fact, selective oxidations could be used in order to produce olefins and oxygenated products like alcohols, carboxylic acids, anhydrides through less expensive processes with lower environmental impact than more traditional processes [1].

Propylene is mainly produced by steam cracking and catalytic dehydrogenation. Non-catalytic steam cracking is widely used in order to produce light olefins (ethylene and propylene). Generally by-products, such as methane, diolefins, acetylene, are co-produced and costly separated from the desired olefins. Moreover, steam cracking needs a large heat supply, due to its high endothermicity and to the elevated operating temperatures (about 850 °C). Although more selective, catalytic dehydrogenation is highly endothermic and is limited by coke production that requires a regeneration step of the deactivated catalyst.

The oxidative dehydrogenation (ODH) of propane is a promising alternative route for the production of propylene, due to several advantages. In particular, (i) heat supply can be significantly reduced because of the intrinsic exothermicity of the ODH reaction; (ii) there is no thermodynamic limitation due to the formation of water and (iii) no coke is produced (or if produced is, then, burnt by oxygen). On the other hand, ODH reaction, like all selective oxidations, suffers from selectivity problems related to the higher reactivity of the product with respect to the reactant, leading to the formation of CO_x [2,3]. From a general point of view, a selective oxidation like ODH is promoted by two different factors: (1) oxygen activation, performed by a redox site, and (2) alkane activation, performed by an acid site through an acid–base interaction with the reactant [4]. Even if the contemporary presence of both types of sites is necessary, Ai underlined that the balance between redox and acid sites is fundamental in order to avoid non-selective pathways, leading to overoxidation or cracking products [4].

Two main classes of catalysts have been proposed for the ODH of propane, both of them containing vanadium as the active phase. The first is constituted by microporous and mesoporous materials with structured or extra-lattice vanadium [5–14]. In this case the catalyst contains a low amount of vanadium, that is well dispersed. The good "site isolation", i.e. the formation of isolated active atoms or small clusters or complexes, is expected to provide an enhanced selectivity [15]. Microporous frameworks could be considered intrinsic "single-site" catalysts, due to the possibility to introduce metal ions into well-defined positions, but, generally, these catalysts do not show high activity due to the low amount of vanadium sites [16].

The second class of catalysts consists of supported or unsupported vanadia or vanadates (usually magnesium vanadates)

* Corresponding author. Tel.: +39 0817682233; fax: +39 0815936936.
E-mail addresses: mariapia.casaletto@ismn.cnr.it (M.P. Casaletto), landi@irc.cnr.it (G. Landi), lisi@irc.cnr.it (L. Lisi), pasquale.patrono@imip.cnr.it (P. Patrono), fulvia.pinzari@imip.cnr.it (F. Pinzari).

1381-1169/$ – see front matter © 2010 Elsevier B.V. All rights reserved.
doi:10.1016/j.molcata.2010.06.017

[17–28]. These catalysts generally show relatively high conversion of propane, depending on the amount of the active phase and the reaction conditions, but propylene yields are limited by a low selectivity to the desired product. In order to obtain better catalytic performance, modifications of the physico-chemical features of the V-containing oxide have been induced by changing catalyst and/or support composition. The use of a TiO_2 layer deposited by grafting [18], the doping with K and/or P and transition metals [21,24,27] can be mentioned as attempts to increase catalytic performances, related to the change of redox and acid properties of the materials.

Bulk vanadyl pyrophosphate (VPO) is industrially used for the production of maleic anhydride starting from n-butane [29–32] and has been proposed for propane selective oxidation to acrylic acid [33–36]. While increasing surface disorder and V^{+5}/V^{+4} ratio are key factors in order to improve maleic anhydride selectivity [37,38], a higher crystallinity and the absence of V^{+5} species lead to better performance of VPO towards acrylic acid formation [35], suggesting that the effect of catalyst modifications on different reactions is not trivial. Recently, bulk VPO, mainly containing V^{+4}, has been proposed as propane ODH catalyst [39], whereas supported vanadyl orthophosphates (VOP), principally constituted by V^{+5}, have been proven to be active and selective in ODH of ethane, titania-supported samples providing the best catalytic performances [40,41]. A deep investigation of these catalysts in ethane ODH has been carried out [40–46], while no information is available on the activity in ODH of propane, which is intrinsically more reactive than ethane and requires lower reaction temperatures.

A strong influence of the support on the properties of the VOP catalysts have been found by XPS studies, which showed that oxides promoting a better VOP dispersion, such as TiO_2, deeply interact with VOP favouring the formation of V(IV) and metal–phosphates compounds [46].

The previous results encouraged us to extend our work to the oxidative dehydrogenation of propane to propylene and, in particular, to focus the aim of this paper on the investigation of which properties of the vanadyl orthophosphate/support system are fundamental in the selective C_3H_8 activation and which modifications of the active phase are induced by the interaction with the support. In order to study that, vanadyl orthophosphate has been deposited onto several supports (TiO_2, γ-Al_2O_3, ZrO_2, SiO_2, MgO, and SnO_2) and tested in the propane ODH reaction. The catalytic activity has been related to the physico-chemical properties of the different materials using several characterization techniques as XRD, BET, H_2-TPR and XPS.

2. Experimental

Vanadyl orthophosphate, $VOPO_4{\cdot}2H_2O$ (VOP), was prepared as described in [41].

γ-Al_2O_3 (CK-300 AKZO), anatase TiO_2 (Eurotitania), amorphous SiO_2 (Sigma), ZrO_2, MgO and SnO_2 were used as supports. ZrO_2, MgO and SnO_2 were prepared by conventional precipitation methods.

In particular, ZrO_2 was prepared by slowly adding a 7.6 M ammonia aqueous solution (Carlo Erba RPE) to an equal volume of 0.1 M $ZrOCl_2{\cdot}8H_2O$ (Carlo Erba RPE) aqueous solution pre-heated at 80 °C under magnetic stirring for 15 h. The final pH was 10. At the end the precipitate was digested for 4 h, washed with distilled water, filtered and dried at 90 °C overnight. Thereafter it was crushed and calcined at 600 °C for 3 h.

MgO was prepared in a similar way. A 6.4 M ammonia water solution was slowly added to a 0.05 M $Mg(NO_3)_2{\cdot}6H_2O$ (Fluka purum ≥99%) aqueous solution under magnetic stirring (without heating); the ratio between ammonia and magnesium containing solution volumes was 4.2. After 1 h stirring the precipitate was digested for 1 h, washed with distilled water, filtered, dried at 90 °C overnight and subsequently crushed and calcined at 600 °C for 3 h.

Finally, SnO_2 was prepared as described in [47]. A 1 M urea (Sigma ACS 99.0–100.5%) aqueous solution was added to a 0.01 M $SnCl_4{\cdot}5H_2O$ (Carlo Erba 98%) aqueous solution and the mixture was heated at 80 °C under magnetic stirring; the ratio between urea and tin containing solution volumes was 25. After 6 h the precipitate was digested for 2 days, washed with distilled water, filtered, dried at 90 °C and calcined at 600 °C for 3 h.

Each support was loaded with a different amount of VOP in order to obtain the deposition of a theoretical monolayer; the proper amount of $VOPO_4$ was calculated taking into account the support specific surface area, as reported in Table 1. The so calculated VOP amounts were dissolved in a little quantity of water, in such a way that the final volume result 2–3 times the support volume. The support was added to the solution, then the mixture was heated under magnetic stirring in order to evaporate the liquid phase, avoiding solution boiling. At the end the material was crushed, further dried at 80 °C, and calcined at 550 °C in flowing air.

All these catalysts are indicated as VOP/M, where M represents the metal ion of the oxide support.

In order to study the effect of the VOP loading, the ZrO_2 support was also loaded with a VOP amount corresponding to five layers; this catalyst was prepared according to the procedure described above by using a five times larger quantity of VOP. This catalyst is indicated as VOP/Zr-5L.

X-ray diffraction patterns of calcined catalysts were recorded by using a Philips PW 1100 diffractometer with Ni-filtered Cu Kα radiation. Angular measurements (2θ) were accurate to 0.05°. BET surface areas were measured by N_2 adsorption at 77 K with a Carlo Erba 1900 Sorptomatic.

Temperature programmed reduction with hydrogen (H_2-TPR) was carried out by using a Micromeritics TPD/TPR 2900 analyser, equipped with a thermal conductivity detector and coupled with a Hiden HPR 20 mass spectrometer, operating with a 2% H_2/Ar mixture (25 $cm^3\,min^{-1}$ flux) and a heating rate of 10 °C min^{-1} up to 630 °C. Samples were treated in flowing air at 550 °C for 2 h before analysis.

The surface chemical composition of the samples was studied by XPS in an ultrahigh vacuum chamber (base pressure $\sim 10^{-8}$ Torr). Photoemission spectra were collected by a VG Microtech ESCA 3000 Multilab spectrometer, equipped with a standard Al Kα excitation source ($h\nu$ = 1486.6 eV), a nine-channeltrons detection system and a hemispherical analyser operating at a constant pass energy of 20 eV. The binding energy (BE) scale was calibrated by measuring C 1s peak (BE = 285.1 eV) from the surface contamination and the accuracy of the measure was ±0.1 eV. A non-linear least-square peak fitting routine was used for the analysis of XPS spectra, separating elemental species in different oxidation states. Relative concentrations of chemical elements were calculated by a standard quantification routine, including Wagner's energy dependence of attenuation length [48] and a standard set of VG Escalab sensitivity factors.

Catalytic activity tests were carried out with the experimental apparatus described elsewhere [41], equipped with a fixed bed quartz reactor operating under atmospheric pressure. The feed composition was 5.2% C_3H_8 and 2.6% O_2 in a balance of N_2. The reaction temperature ranged from 300 to 500 °C. The contact time ranged from 0.003 to 0.08 g h N dm^{-3}. The reaction products were analysed with a Hewlett Packard series II 5890 gas-chromatograph, equipped with a thermal conductivity detector for O_2, CO and CO_2 analysis and a flame ionization detector for hydrocarbons analysis. The concentrations of O_2, CO and CO_2 were also measured on line with a Hartmann & Braun URAS 10 E continuous analyser. Water produced during reaction was kept apart by a silica gel trap in order to avoid condensation in the cold part of the experimen-

Table 1
Nominal VOP content, surface area of catalysts and supports and H_2/V ratio evaluated from TPR experiments.

Catalyst	Nominal VOP content (wt%)	Support surface area ($m^2\ g^{-1}$)	Catalyst surface area ($m^2\ g^{-1}$)	H_2/V from TPR	
				Fresh	React.
VOP-Ti	9.6	125	125	0.71	0.63
VOP-Al	14.0	190	183	0.67	0.55
VOP-Si	14.6	200	162	0.51	–
VOP-Zr	3.6	49	43	1.07	0.86
VOP-Mg	7.8	105	56	0.63	–
VOP-Sn	2.6	34	31	1.0	–
VOP-Zr-5L	18.2	49	27	0.71	–

tal apparatus. Carbon balance was closed within 3% error in all experiments. Blank tests performed under the same experimental conditions excluded the occurrence of homogenous reactions. The results reported below are only catalytic or catalytically induced.

3. Results

In Table 1 the nominal VOP content and the surface area of both supports and catalysts are reported. A general reduction of the original surface area of the support occurs upon deposition of VOP, titania- and alumina-based catalysts showing the less significant decrease. A further reduction of the surface area was observed in the VOP-Zr-5L sample due to the great excess with respect to the VOP monolayer content.

XRD patterns of selected samples are reported in Fig. 1. Among monolayer catalysts the presence of segregated VOP phase is detected on SnO_2 supported sample, as shown by the main signal of vanadyl hydrogen phosphate hemihydrate at $2\theta = 15.48^\circ$ [49]. SiO_2 and MgO supported samples, whose spectra are not reported, show a similar behaviour. On the contrary no evidence of VOP signals has been detected on the other samples, suggesting the absence of VOP segregation, as indicated by the patterns of TiO_2- and ZrO_2-supported catalysts reported in Fig. 1. Weak signals of VOP were also observed for VOP-Zr-5L.

All catalysts can convert propane although with different activity, while bulk VOP activity towards propane ODH is undetectable under experimental conditions comparable to those used for supported catalysts. This behaviour is not surprising taking into account our previous results on the ethane ODH [43]. Among supported samples, two main behaviours towards propane oxidation can be detected under the investigated experimental conditions. For VOP supported on titania, alumina, zirconia and silica the main product is propylene in the whole range of investigated temperatures whereas CO_2 represents the most abundant product for MgO and SnO_2 supported catalysts. The behaviour of VOP/Mg is not surprising; as a matter of fact, Klisinska et al. [27] reported that magnesia supported vanadium exhibits higher selectivity to CO_2 than propylene. In Fig. 2 the different behaviour of the two classes of catalysts, represented by VOP/Ti (Fig. 2a) and VOP/Sn (Fig. 2b), respectively, is compared. For VOP/Ti the decrease of propylene formation is mainly balanced by the oxidation to CO and CO_2, as also reported for ethane ODH [41]. For VOP/Sn formation of CO_2 slightly decreases with temperature, whereas production of CO is activated

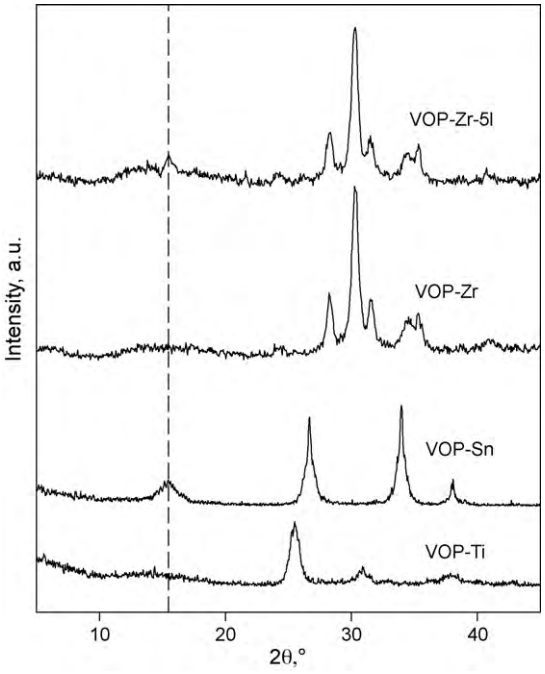

Fig. 1. XRD patterns of different supported VOP catalysts. Vertical lines indicates main VOP reflections.

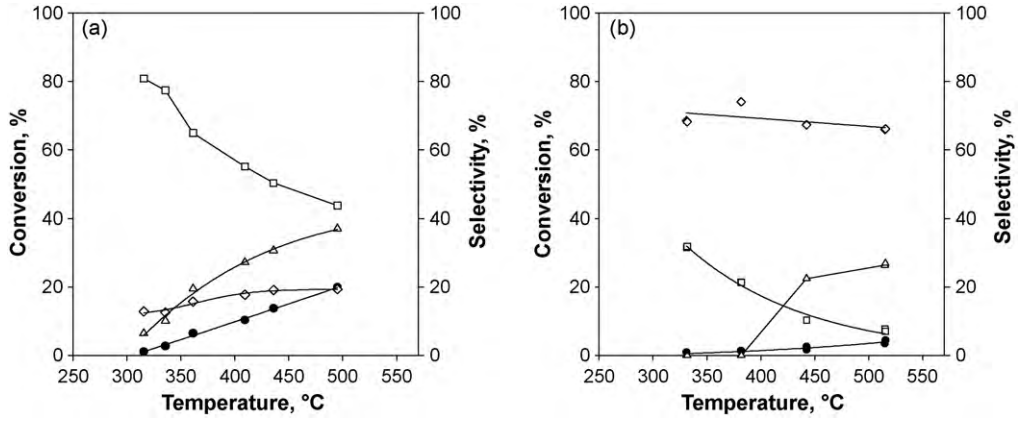

Fig. 2. Propane conversion (●) and propylene (□), CO (Δ) and CO_2 (◊) selectivity as a function of reaction temperature on VOP/Ti (a) and VOP/Sn (b).

Table 2
Values of propane converted per mass and SSA of catalyst and per vanadium atom (TOF) and of propylene produced per vanadium atom (TOF_2) at 450 °C.

Catalyst	Reaction rate[a]	Reaction rate[b]	TOF[c]	TOF_2[d]	Active sites[e]
VOP-Ti	10.3	8.2	1.7	0.94	2.86
VOP-Al	4.7	2.5	0.6	0.36	2.85
VOP-Zr	2.2	4.5	1.0	0.66	3.35
VOP-Si	0.2	0.1	0.03	0.02	3.11
VOP-Mg	0.6	0.6	0.1	0.02	5.18
VOP-Sn	0.3	0.9	0.2	0.02	3.12
VOP-Zr-5L	4.6	9.4	0.4	0.26	25.1

[a] $Mol_{C3H8}\ g^{-1}\ s^{-1} \times 10^6$.
[b] $Mol_{C3H8}\ m^{-2}\ s^{-1} \times 10^4$.
[c] $Mol_{C3H8}\ mol_V^{-1}\ s^{-1} \times 10^2$.
[d] $Mol_{C3H6}\ mol_V^{-1}\ s^{-1} \times 10^2$.
[e] Number $m^{-2} \times 10^{18}$ (on the basis of catalyst surface area).

only at $T \geq 450$ °C, globally resulting in a decrease of propylene selectivity with propane conversion. In Table 2 the values of reaction rate evaluated at 450 °C and referred to catalyst weight, surface area and vanadium content (Turnover frequency – TOF), under the hypothesis of differential reactor, are reported. VOP/Ti shows the best performance, whereas VOP/Si, VOP/Mg and VOP/Sn show an activity at least one order of magnitude lower. Only in terms of specific surface area VOP/Zr-5 shows an activity comparable to that of VOP/Ti, but with a vanadium content about double.

The high activity of VOP/Ti is confirmed by comparing the performance of the most active catalysts as a function of contact time (Fig. 3) at a fixed temperature of 450 °C. Very low contact times are required by VOP/Ti in order to convert propane; in particular, 10% propane conversion with 60% propylene selectivity is obtained at only about 4 ms residence time, calculated at the reaction temperature. This results in a very high TOF, as reported in Table 2. The difference among catalysts behaviour is not attributable to the generation of different active sites onto the different supports. As a matter of fact, for these catalysts the selectivity to propylene seems basically related to propane conversion independently of the support (Fig. 4), thus suggesting that the active sites have the same nature, while the active species of low activity catalysts appears different, corresponding points in Fig. 4 being far from the line associated to the best catalysts. The best active centres are also able to activate both propane and propylene, and, as a consequence, at high contact times, i.e. at higher C_3H_8 conversion, the olefin is further oxidized to CO_x (Fig. 4).

In Fig. 5 the effect of VOP loading on zirconia support is reported in terms of propane conversion versus propylene selectivity. As can

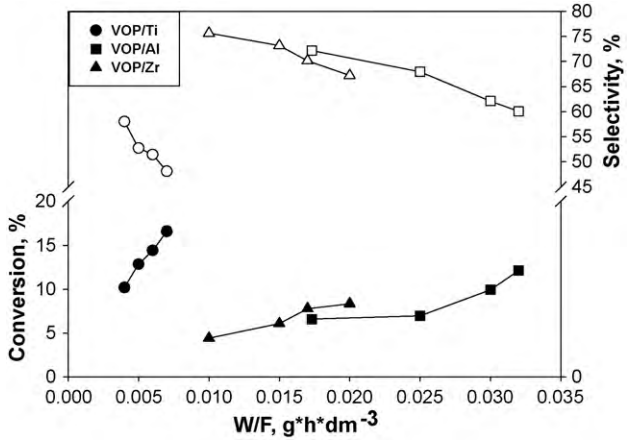

Fig. 3. Propane conversion (full symbols) and propylene selectivity (open symbols) at 450 °C as a function of contact time for VOP/Ti, VOP/Al and VOP/Zr catalysts.

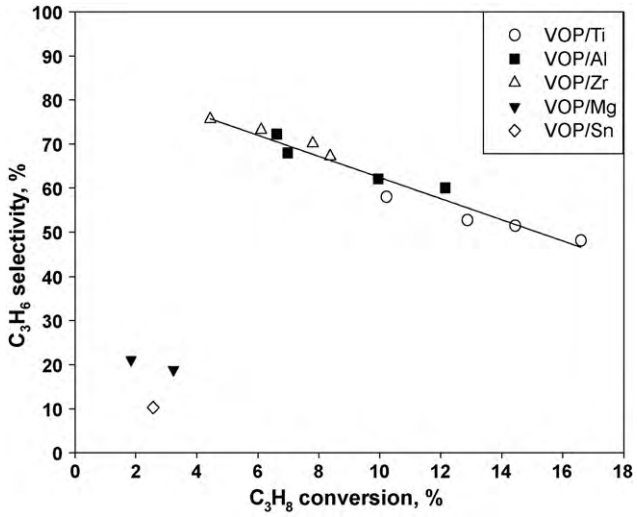

Fig. 4. Propylene selectivity as a function of propane conversion for VOP/M catalyst (T = 450 °C; W/F = 0.003–0.08 g h N dm^{-3}).

be noted, the two plots show a different slope. In particular, in the multilayer catalyst propylene selectivity extrapolated to zero conversion approaches 100%, whilst is about 80% for the monolayer VOP/Zr catalyst. On the other hand, in this catalyst propylene selectivity is less affected by the increase of propane conversion, thus suggesting the presence of sites promoting a different reaction pathway. It seems that on the monolayer VOP/Zr propylene oxidation to CO_x is less temperature-sensitive, thanks to the formation of different active sites, which prevent propylene overoxidation. TOF values of the two zirconia-based catalysts, reported in Table 2, indicates that some VOP segregation should take place in the VOP/Zr-5L sample, which markedly reduces the exposure of vanadium species, as confirmed by XRD analysis.

The relative surface chemical composition of the samples determined by XPS is reported in Table 3. Elemental concentrations are expressed as atomic percentage (at.%) and calculated both before and after ODH test.

VOP/Ti catalyst exhibits the highest surface vanadium concentration (see P/V ratios in Table 3), which could be related to its good activity in propane ODH. Nevertheless, some surface phosphorous enrichment occurs upon reaction test.

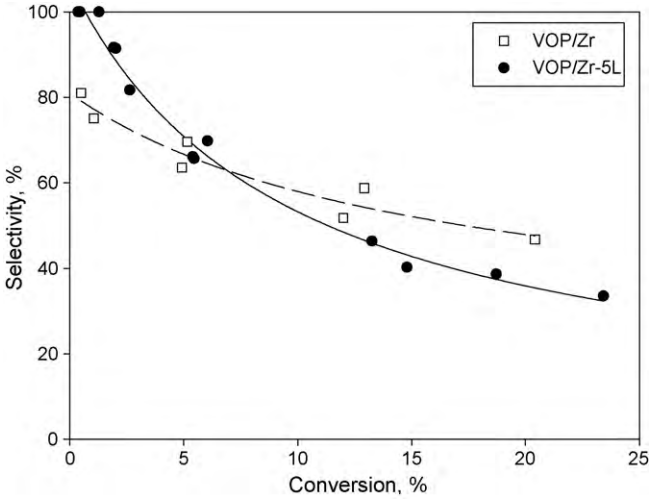

Fig. 5. Propylene selectivity as a function of propane conversion evaluated at different temperatures for VOP/Zr and VOP/Zr-5L catalysts (W/F = 0.02–0.08 g h dm^{-3}; T = 300–550 °C).

Table 3
XPS relative surface chemical composition (expressed in atomic %) of catalysts after calcination and ODH tests.

Catalyst	V $2p_{3/2}$	O 1s	P 2p	Support ion	P/V	O/P
VOP/Ti						
Dried	2.7	75.5	2.7	19.2	1.0	28.0
Calcined at 550 °C	2.5	78.4	2.6	16.5	1.0	30.2
Propane ODH at 450 °C	2.0	71.8	3.1	23.2	1.6	23.2
VOP/Al						
Dried	1.8	61.0	2.5	34.7	1.4	24.4
Calcined at 550 °C	1.3	60.8	2.1	35.8	1.6	29.0
Propane ODH at 450 °C	1.2	65.4	1.8	31.5	1.5	36.3
VOP/Zr						
Dried	1.7	70.4	2.7	25.2	1.6	26.1
Calcined at 550 °C	1.9	67.5	2.9	27.7	1.5	23.3
Propane ODH at 450 °C	1.5	69.2	2.4	26.9	1.6	28.8
VOP/Zr-5L						
Dried	5.1	70.3	8.3	16.4	1.6	8.5
Calcined at 550 °C	5.2	69.4	7.3	18.1	1.4	9.5

Also the O/P atomic ratio is reported in Table 3, even if the investigated samples consisted of vanadyl phosphates supported on different oxidic matrixes (and not pure compounds) that underwent different interactions with the support through the oxygen atom. Since XPS detects only the surface chemical composition of the samples (not necessarily corresponding to the bulk), the stoichiometric ratio of the pure vanadyl phosphate phase cannot be found and, as determined by XPS quantitative analysis in Table 3, an extraordinarily predominance of oxygen atoms is detected (O/P ratio ~25–30). Significant is the reduction of the O/P ratio in the VOP/Zr-5L sample where the amount of vanadyl phosphates on the surface of ZrO_2 exceeded so much the monolayer coverage.

XPS profiles of the V $2p_{3/2}$ photoelectron peak in VOP/Ti, VOP/Al and VOP/Zr samples are reported in Fig. 6(a)–(c), respectively. At a first visual inspection, a shoulder at high binding energy value is clearly distinguishable in the V $2p_{3/2}$ spectrum of VOP/Ti sample in Fig. 6a. This shoulder is totally absent in the XPS profile of the VOP/Zr sample (Fig. 6b).

The results of the curve-fitting procedure of the V $2p_{3/2}$ photoelectron peak in VOP/Ti and VOP/Al samples evidenced the presence of three components at BE = 518.2, 516.9 and 515.8 eV, which can be assigned to V^{5+} phosphate species as detected in $VOPO_4$, to V^{5+} oxide species as in V_2O_5 and to V^{4+} oxide species as in V_2O_4, respectively [41,50]. In the VOP/Zr sample only the last two components are present. As reported in [45], dispersion of VOP on TiO_2 or Al_2O_3 results in the formation of a significant amount of V^{5+} and V^{4+} oxides, since a fraction of phosphorous preferentially interacts with the support leading to the formation of titanium or aluminium phosphate, respectively. A fraction of V^{4+} species is formed even at low temperature in the dried samples. Calcination at 550 °C under oxidizing atmosphere surprisingly promotes a further reduction of vanadium, as evidenced by the increase of the V^{4+} fraction, as also reported in [46]. This reduction is accompanied by the interaction of phosphorous with the support ions, leading to the formation of a larger fraction of titanium or aluminium phosphate, and by the decrease of the amount of vanadium phosphate (Table 4). In other words, calcination mainly favours the migration of phosphate ions from vanadium to the support, generating an additional fraction of V(IV) oxide. The interaction of phosphorous oxide with both V_2O_5 and TiO_2 was also reported by Deo and Wachs [51] who observed the formation of $VOPO_4$ by addition of P_2O_5 to V_2O_5/TiO_2 catalyst and the formation of vanadium–oxygen–phosphorous bonds by deposition of V_2O_5 to a previously prepared P_2O_5/TiO_2 sample. This phenomenon was not observed for supports which do not promote the formation of

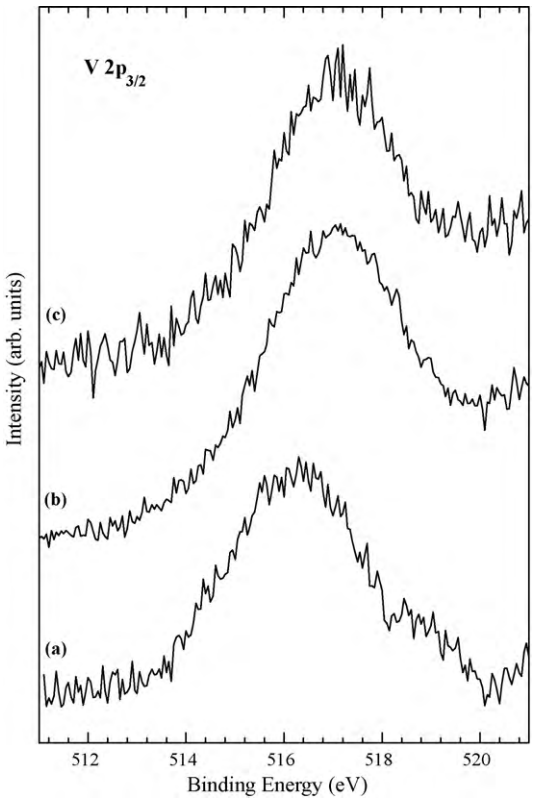

Fig. 6. XPS profiles of VOP/Ti (a), VOP/Al (b) and VOP/Zr (c) catalysts in the energy range of V 2p3/2 photoelectron peak.

vanadium phosphate, such as in VOP/Zr catalysts. In this case the calcination process favours the oxidation of V(IV) oxide species to V(V) oxide, as expected under oxidizing atmosphere.

Zr 3d peak is located at a quite constant binding energy value in both VOP/Zr catalysts (BE = 183.1 eV), attributable to Zr^{4+} ions as in ZrO_2 [48]. This was further confirmed by the curve-fitting of O 1s peak, which can be deconvoluted into three components at BE = 530.5, 531.7 and 533.2 eV, assigned to oxide, hydroxide and/or phosphate species, and to adsorbed water, respectively [50]. The main component of the O 1s peak (75% peak area) is that related to oxide species (BE = 530.5 eV), The predominance of the oxide support peak in the XPS spectrum could be attributed to a bad VOP surface distribution with a consequent exposure of significant fraction of the support surface.

In the dried multilayer VOP/Zr-5L sample the binding energy of Zr 3d shifts towards a slightly higher value that could hint to an initial interaction between VOP and ZrO_2 finally leading to the formation of $Zr(HPO_4)_2$ species [52]. The main component of O 1s peak was located at BE = 531.7 eV, corresponding to the presence of OH^- groups and O–P bonds, as expected due to the greater VOP concentration of this catalyst. Nevertheless, formation of oxides species prevails on that of phosphates upon calcination, as shown by the lower binding energy value of Zr 3d peak (as in the monolayer catalyst) and the predominance of the component attributed to the oxide (BE = 530.5 eV) in the curve-fitting of the O 1s peak (62% peak area).

Redox properties of these materials are deeply involved in the reaction mechanism [44,45]. Therefore, a TPR analysis was carried out in order to explain the large difference of activity observed for the investigated samples. In Fig. 7 the TPR profiles of VOP/Ti, VOP/Al and VOP/Zr are compared with that of bulk VOP. Dispersion of VOP results into a significant enhancement of reducibility, which is maximum for TiO_2 support. On the other hand, reduction

Table 4
XPS relative surface distribution (expressed as peak area %) of different vanadium species in catalysts after calcination and ODH tests.

Catalyst	V^{5+} phosphate	V^{5+} oxide	V^{4+} oxide	Support ion oxide	Support ion phosphate
VOP/Ti					
Dried	13.8	49.3	36.9	83.7	16.3
Calcined at 550 °C	13.2	42.5	44.3	65.3	34.7
Propane ODH at 450 °C	7.6	61.4	31.0	23.8	76.2
VOP/Al					
Dried	40.0	56.0	4.0	~100	n.d[a]
Calcined at 550 °C	31.1	52.4	16.5	93.2	6.8
Propane ODH at 450 °C	20.3	56.3	23.4	19.8	80.2
VOP/Zr					
Dried	n.d[a]	49.5	50.5	~100	n.d[a]
Calcined at 550 °C	n.d[a]	59.6	40.4	~100	n.d[a]
Propane ODH at 450 °C	n.d[a]	44.1	55.9	~100	n.d[a]

[a] Not detectable.

of VOP/Sn and VOP/Mg catalysts (Fig. 8) mainly takes place during the isothermal step of the experiment (630 °C), thus suggesting the presence of hardly reducible bulk-like VOP. Moreover, as suggested by the TPR profile of VOP/Sn, a significant support reduction occurs, not allowing a precise calculation of H_2/V ratio (Table 1). On the other hand, this catalyst shows combustion rather than ODH activity, strongly suggesting that the support contributes to CO_x formation. These results confirm that vanadium reducibility is a key feature for hydrocarbon selective oxidation, while other metal sites are active in non-selective pathways. The H_2/V ratio of the best catalysts, except VOP/Zr, lower than the stoichiometric value of 1 expected for the reduction from V^{5+} to V^{3+}, are in good agreement with the presence of a fraction of vanadium in 4+ oxidation state, as found by XPS analysis. The H_2 uptake of the ZrO_2-supported monolayer catalyst can be affected by a slight support reduction, thus leading to H_2/V higher than 1, even in the presence of a V^{4+} fraction as revealed by XPS measurements. The exposure to the reacting environment produces a further reduction, i.e. an increase of the V^{4+} fraction, as reported in Table 1, suggesting once more that vanadium redox cycles are responsible for propane ODH.

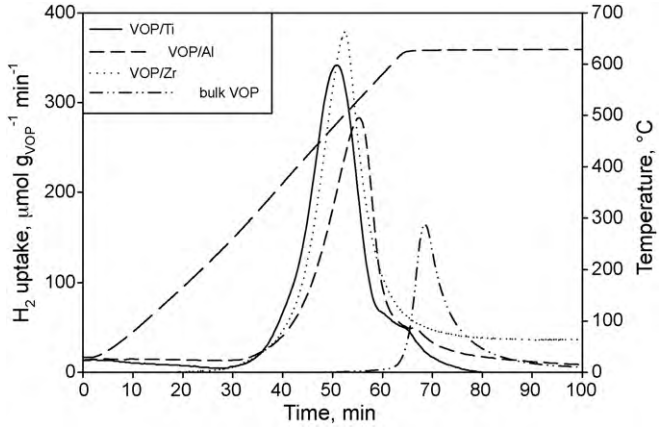

Fig. 7. TPR profiles of VOP/Ti, VOP/Al and VOP/Zr catalysts compared with that of bulk VOP.

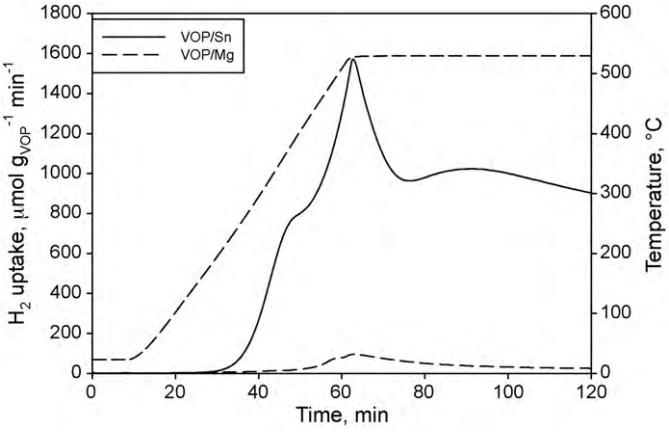

Fig. 8. TPR profile of VOP/Sn and VOP/Mg catalysts

Moreover, XPS analysis carried out on the catalysts after the catalytic test at 450 °C (Table 4) suggests that the ODH reaction promotes a redistribution of surface species. For both VOP/Ti and VOP/Al a fraction of vanadium phosphate, initially present in the fresh sample, is transformed into vanadium oxide and, at the same time, the fraction of titanium or aluminium phosphate increases, thus suggesting that the catalytic tests promotes a further migration of phosphorous from vanadium to the support. Since the catalytic test was carried out at a lower temperature with respect to that of calcination, these results suggest that the interaction of phosphate ion with the support is favoured by a redox cycle of vanadium rather than by high temperatures. Due to the low amount of active phase, the identification of phosphate species, related to the superficial phosphorus (Table 3), on VOP/Zr surface resulted difficult.

4. Discussion

The results reported above clearly demonstrate that the activity of VOP-based catalysts strongly depends on the support. In particular, the formation of superficial phosphates including metal phosphates of the support, as detected by XPS measures, seems the key factor to obtain highly active vanadium species. Indeed, the samples showing this strong interaction between the active phase and the support are characterized by very low reduction of the surface area after VOP deposition, suggesting the formation of very highly dispersed vanadium-containing species undetectable by XRD analysis. On the contrary, the samples providing the worst performances, are those in which most vanadium centres are inactive because of the formation of VOP aggregates, as detected by XRD, causing significant surface area reduction as well. Due to the typical redox nature of the investigated reaction, another key point is the increased reducibility of vanadium centres, as revealed by TPR measures; the increased reducibility, in fact, is directly related to the enhanced TOF showed by highly active catalysts. Moreover, this behaviour appears more related to the high dispersion of the vanadia species than to the reducibility of the support; as a matter of fact, the high reducibility of VOP/Sn is not coupled with a high ODH activity, but more related to a undesired combustion activity. The behaviour of multilayer VOP/Zr can be explained according to

the above considerations; the presence of larger amounts of active phase leads to a better coverage of the surface, avoiding the propane reaction with the ZrO_2 centres directly, and, as a consequence, the selectivity towards ODH reaction approaches 100% for zero conversion. On the other hand, the higher reducibility of larger vanadium cluster obtained on the multilayer catalyst favours the propylene overoxidation and results in lower catalytic performance at relatively higher propane conversion. Finally, the highest TOF are not related to the highest support surface area, as revealed by the low performance of VOP/Si. In conclusion, the high dispersion of the active phase and, as a consequence, the increased reducibility and TOF towards C_3H_8 ODH can be uniquely related to the capability of the support to strongly interact with the active phase. As it can be derived from the above results and considerations, the active phase obtained on our samples is constituted by small clusters of vanadium oxide; this is the same active phase obtained for vanadia supported catalysts [53]. With respect to these catalysts, VOP-based ones show about the same activity towards propane but an enhanced selectivity towards propylene. This is due to the better dispersion of vanadium centres induced by the formation of metal phosphates of the support, leading to more selective active centres.

5. Conclusions

The study of the oxidative dehydrogenation of propane has been conducted over vanadyl orthophosphate based catalysts supported onto TiO_2, γ-Al_2O_3, ZrO_2, SiO_2, MgO and SnO_2. According to XRD, BET and XPS measurements, the best performing catalysts, supported on TiO_2, ZrO_2 and γ-Al_2O_3, have a good active phase dispersion and a strong interaction between phosphate and substrate, evidenced by low reduction in the surface area upon VOP deposition and the formation of a well dispersed superficial vanadium oxide layer in addition to vanadium phosphate. On the contrary, VOP segregation is correlated to a low activity and to the formation of CO_2 as the main product. H_2-TPR and XPS measurements allowed us to correlate the catalytic activity to the enhanced vanadium reducibility, suggesting that an easier reducibility of the active phase is fundamental for high propylene production.

References

[1] F. Cavani, F. Trifirò, Catal. Today 51 (1999) 561.
[2] J.M. Thomas, Angew. Chem. Int. Ed. 38 (1999) 3588.
[3] J.M. López Nieto, Top. Catal. 41 (1–4) (2006) 3.
[4] M. Ai, Kinet. Catal. 44 (2) (2003) 198.
[5] G. Centi, F. Trifirò, Appl. Catal. A: Gen. 143 (1996) 3.
[6] A. Kubacka, E. Wloch, B. Sulikowski, R.X. Valenzuela, V. CortèsCorberàn, Catal. Today 61 (2000) 343.
[7] Z.-S. Chao, E. Ruckenstein, Catal. Lett. 94 (2004) 217.
[8] B. Solsona, T. Blasco, J.M. López Nieto, M.L. Peña, F. Rey, A. Vidal-Moya, J. Catal. 203 (2001) 443.
[9] J. Santamaria-González, J. Luque-Zambrana, J. Mérida-Robles, J. Maireles-Torres, E. Rodríguez-Castellón, A. Jiménez-López, Catal. Lett. 68 (2000) 67.
[10] E.V. Kondratenko, M. Cherian, M. Baerns, D. Su, R. Schlögl, X. Wang, I.E. Wachs, J. Catal. 234 (2005) 131.
[11] A. Brueckner, P. Rybarczyk, H. Kosslick, G.-U. Wolf, M. Baerns, Stud. Surf. Sci. Catal. 142B (2002) 1141.
[12] Y.M. Liu, Y. Cao, K.K. Zhu, S.R. Yan, W.L. Dai, H.Y. He, K.N. Fan, Chem. Commun. 23 (2002) 2832.
[13] Y.M. Liu, Y. Cao, N. Yi, W.L. Feng, W.L. Dai, S.R. Yan, H.Y. He, K.N. Fan, J. Catal. 224 (2004) 417.
[14] B. Solsona, J.M. López Nieto, U. Díaz, Micropor. Mesopor. Mater. 94 (2006) 339.
[15] J.-C. Volta, Top. Catal. 15 (2–4) (2001) 121.
[16] J.M. Thomas, R. Raja, Top. Catal. 40 (2006) 3.
[17] F. Genser, S. Pietrzyk, Chem. Eng. Sci. 54 (1999) 4315.
[18] R. Monaci, E. Rombi, V. Solinas, A. Sorrentino, E. Santacesaria, G. Colon, Appl. Catal. A: Gen. 214 (2001) 203.
[19] B.Y. Jibril, S.M. Al-Zahrani, A.E. Abasaeed, Catal. Lett. 74 (2001) 145.
[20] A. Comite, A. Sorrentino, G. Capannelli, M. Di Serio, R. Tesser, E. Santacesaria, J. Mol. Catal. A: Chem. 198 (2003) 151.
[21] G. Garcia Cortez, J.L.G. Fierro, M.A. Bañares, Catal. Today 78 (2003) 219.
[22] M.J. Holgado, F.M. Labajos, M.J.S. Montero, V. Rives, Mater. Res. Bull. 38 (2003) 1879.
[23] S. Sugiyama, T. Hashimoto, N. Shigemoto, H. Hayashi, Catal. Lett. 89 (2003) 229.
[24] A. Klisińska, A. Haras, K. Samson, M. Witko, B. Grzybowska, J. Mol. Catal. A: Chem. 210 (2004) 87.
[25] J.D. Pless, B.B. Barsin, H.-S. Kim, D. Ko, M.T. Smith, R.R. Hammond, P.C. Stair, K.R. Poeppelmeier, J. Catal. 223 (2004) 419.
[26] A. Christodoulakis, M. Machli, A.A. Lemonidou, S. Boghosian, J. Catal. 222 (2004) 293.
[27] A. Klisińska, K. Samson, I. Gressel, B. Grzybowska, Appl. Catal. A: Gen. 309 (2006) 10.
[28] G. Martra, F. Arena, S. Coluccia, F. Frusteri, A. Parmaliana, Catal. Today 63 (2–4) (2000) 197.
[29] R.M. Contractor, US Patent 4,668,802 (1987), to DuPont.
[30] G.D. Suciu, G. Stefani, C. Fumagalli, US Patent 4,511,670 (1985), to Lummus Crest Inc. and Alusuisse Italia SpA.
[31] H. Taheri, US Patent 5,011,945 (1991), to Amoco Co.
[32] G.K. Kwentus, M. Suda, US Patent 4,501,907 (1985), to Monsanto Co.
[33] G. Landi, L. Lisi, J.-C. Volta, Chem. Commun. 4 (2003) 492.
[34] G. Landi, L. Lisi, J.-C. Volta, Catal. Today 91–92C (2004) 275.
[35] G. Landi, L. Lisi, J.-C. Volta, J. Mol. Catal. A: Chem. 222 (2004) 175.
[36] G. Landi, L. Lisi, G. Russo, J. Mol. Catal. A: Chem. 239 (2005) 172.
[37] M. Abon, K.E. Bere, A. Tuel, P. Delichere, J. Catal. 156 (1995) 28.
[38] K. Aït-Lachgar, A. Tuel, M. Brun, J.M. Herrmann, J.M. Krafft, J.R. Martin, J.C. Volta, M. Abon, J. Catal. 177 (1998) 224.
[39] S. Arias-Pérez, R. García-Alamilla, M.G. Cárdenas-Galindo, B.E. Handy, S. Robles-Andrade, G. Sandoval-Robles, Ind. Eng. Chem. Res. 48 (2009) 1215.
[40] M.P. Casaletto, S. Kaciulis, L. Lisi, G. Mattogno, A. Mezzi, P. Patrono, G. Ruoppolo, Appl. Catal. A: Gen. 218 (2001) 129.
[41] M.P. Casaletto, L. Lisi, G. Mattogno, P. Patrono, G. Ruoppolo, G. Russo, Appl. Catal. A: Gen. 226 (2002) 41.
[42] P. Ciambelli, L. Lisi, P. Patrono, G. Ruoppolo, G. Russo, Catal. Lett. 82 (3–4) (2002) 243.
[43] L. Lisi, P. Patrono, G. Ruoppolo, J. Mol. Catal. A: Chem. 204–205 (2003) 609.
[44] M.P. Casaletto, L. Lisi, G. Mattogno, P. Patrono, G. Ruoppolo, Appl. Catal. A: Gen. 267 (1–2) (2004) 157.
[45] M.P. Casaletto, L. Lisi, G. Mattogno, P. Patrono, F. Pinzari, G. Ruoppolo, Catal. Today 91–92 (2004) 271.
[46] M.P. Casaletto, L. Lisi, G. Mattogno, P. Patrono, G. Ruoppolo, Surf. Interface Anal. 36 (8) (2004) 737.
[47] K.C. Song, Y. Kang, Mater. Lett. 42 (2000) 283.
[48] C.D. Wagner, L.E. Davis, W.M. Riggs, Surf. Interface Anal. 2 (1986) 53.
[49] A.A. Rownaghi, Y.H. Taufiq-Yap, F. Rezaei, Chem. Eng. J. 155 (2009) 514.
[50] J.F. Moulder, W.F. Stickle, P.E. Sobol, K.D. Bomben, in: J. Chastain, R.C. King Jr. (Eds.), Handbook of X-Ray Photoelectron Spectroscopy, Phys. Electronics Inc., Eden Prairie, USA, 1995.
[51] G. Deo, I.E. Wachs, J. Catal. 146 (1994) 335.
[52] L. Lisi, G. Ruoppolo, M.P. Casaletto, P. Galli, M.A. Massucci, P. Patrono, F. Pinzari, J. Mol. Catal. A: Chem. 232 (1–2) (2005) 127.
[53] P. Viparelli, P. Ciambelli, L. Lisi, G. Ruoppolo, G. Russo, J.C. Volta, Appl. Catal. A 184 (1999) 291.